FUZZY LOGIC BASED EV CHARGING CONTROL FOR FREQUENCY REGULATION IN WIND-DIESEL ISLANDED POWER SYSTEMS

YERRAJERLA SUNITHA[1], MRS. U. LAKSHMI [2]

[1] Student, Department of Electrical and Electronics Engineering, Sanketika Vidya Parishad Engineering College, Pothinamallayya Palem (P.M. Palem), Visakhapatnam, Andhra Pradesh, India– 530041
Email: sunithapvs1234@gmail.com

[2] Assistant Professor, Department of Electrical and Electronics Engineering, Sanketika Vidya Parishad Engineering College, Pothinamallayya Palem (P.M. Palem), Visakhapatnam, Andhra Pradesh, India– 530041
India– 530041Email: Ulakshmi27795@gmail.com

ABSTRACT

Growing wind generation in small isolated power systems displaces synchronous diesel units, lowers the rotating inertia and injects a continuous stochastic disturbance into the generation–demand balance, so that the frequency becomes highly sensitive to wind gusts and the fixed-gain proportional–integral (PI) diesel governor struggles to keep it inside the regulatory band. Responsive charging of electric vehicles (EVs) has been proposed as a demand-side resource that can modulate its consumption according to the locally measured frequency, and earlier work on the wind–diesel system of San Cristóbal Island (Galápagos) showed that proportional, soft and aggressive EV strategies using less than 2.5 % of the demand substantially improve the frequency, while retaining the PI governor.

This thesis extends that work by replacing the PI governor of the diesel generation with a Mamdani-type fuzzy logic controller (FLC). The controller uses the frequency deviation and its rate of change as inputs, seven triangular membership functions per variable, a 49-rule base, min–max inference and centroid defuzzification, and is arranged in an incremental (PI-type) structure with an additional proportional path so that zero steady-state error is preserved. The complete system — a 3 × 813 kVA diesel plant, a wind farm of three 800 kW doubly-fed induction generators driven by measured high-resolution wind records, induction-motor, constant-impedance and constant-power loads, and a 50 kW controllable EV charging aggregate — is modelled in MATLAB/Simulink. Thirty-two 600 s wind-profile cases (four wind profiles, four EV strategies, two governors) and three transient events are simulated, and compared through extreme frequencies, standard deviation, time within 60 ± 0.15 Hz, settling time and integral absolute error. The simulation results show that the fuzzy governor reduces the standard deviation of frequency by 54–74 % with respect to the PI governor for every wind profile and EV strategy. For the most demanding profile (high wind speed, high turbulence) the fraction of time inside the acceptable band rises from 27.4 % to 56.8 % without EV participation and from 56.4 % to 75.5 % with aggressive EV control. After the loss of two wind turbines the frequency nadir improves from 58.64 Hz to 59.38 Hz, and the peak deviation after a 100 kW load step is reduced by about 60 %. The improvement is maintained when the system inertia, engine dead time and load damping are varied. Combining a fuzzy governor with low-cost EV demand response is thus an effective route to secure frequency control in isolated grids with high wind penetration.

Keywords: frequency control, fuzzy logic controller, electric vehicles, demand response, isolated power system, wind power, diesel generator, MATLAB/Simulink.

1.INTRODUCTION

1.1 Background

Electrical power systems around the world are undergoing a structural change. Driven by the need to reduce greenhouse-gas emissions, to improve energy security and to lower the cost of electricity, a large share of new generating capacity is provided by renewable energy sources (RES), principally wind and solar photovoltaic plants [1]. This trend is particularly attractive for small isolated systems such as islands, remote mining sites and rural micro-grids, where electricity has traditionally

been produced by diesel generators whose fuel must be transported at high cost and with a significant environmental risk. Replacing part of the diesel production with local wind energy reduces fuel consumption, emissions and the dependence on fuel logistics.

The integration of wind power into small grids is not free of difficulty. Two physical features of wind generation challenge the conventional way in which power systems are operated. First, wind turbines are connected to the grid through power-electronic converters or, in the case of doubly-fed induction generators (DFIG), through a partially rated converter in the rotor circuit [2]. Their rotating masses are therefore decoupled from the electrical frequency, and every megawatt of wind generation that displaces a synchronous diesel unit removes kinetic energy that would otherwise oppose frequency changes [3, 4]. Second, the primary energy source is variable: natural gusts and turbulence cause the output of a wind farm to fluctuate over time scales from seconds to minutes [5, 6]. In a large interconnected network these fluctuations are absorbed by thousands of generators and are statistically smoothed, but in an isolated system of a few megawatts they appear directly as a power imbalance that must be compensated by the few diesel units in service.

The variable that reveals the balance between generation and demand is the system frequency. Its behaviour is governed by the swing equation, which states that any difference between the mechanical power delivered by the generators and the electrical power consumed by the loads is stored in, or taken from, the kinetic energy of the rotating masses [7, 8]. A lower inertia and a larger, noisier imbalance therefore produce faster and larger frequency deviations. Fig. 1.1 illustrates the typical sequence of an underfrequency event: the inertial response determines the initial rate of change of frequency (RoCoF), the primary control of the governors arrests the decline at the frequency nadir, and secondary control restores the nominal value.

2.LITERATURE REVIEW

2.1 Introduction

This chapter reviews the published work that forms the basis of the thesis. The review is organised in five themes: the impact of wind power on the frequency of isolated systems; conventional governor and load frequency control; demand-side and EV participation in frequency regulation; fuzzy logic based frequency control; and the specific studies on the San Cristóbal Island system. The chapter closes with a summary table and the research gap addressed in the following chapters.

2.2 Impact of Wind Integration on Frequency Stability

The technical challenges of integrating wind energy into electricity systems were reviewed by Ibrahim *et al.* [1], who identified power quality, frequency and voltage regulation, and the reduction of system inertia as the main obstacles to high penetration levels. Slootweg and Kling [5] analysed the effect of large-scale wind generation on electromechanical oscillations and showed that variable-speed turbines do not contribute to the damping of frequency-related modes in the same way as synchronous machines. Ackermann's handbook [6] and the wind energy handbook of Burton *et al.* [26] describe the stochastic nature of wind power, the role of turbulence intensity and the smoothing effect of geographically distributed turbines, which is weak in a small wind farm whose turbines are only a few hundred metres apart.

The decoupling of converter-interfaced generation from the grid frequency was analysed in detail by Ekanayake and Jenkins [27], who compared fixed-speed and doubly-fed induction generators and found that the DFIG provides almost no inertial response unless an additional control loop is added. Morren *et al.* [28] proposed such a loop to emulate inertia and support primary frequency control, at the cost of temporary energy extraction from the rotor. Ulbig *et al.* [3] and Tielens and Van Hertem [4] quantified the consequences of low rotational inertia: higher RoCoF, deeper nadirs and a reduced time available for primary controllers to act. These effects are most severe in islanded systems, where the total inertia is small even before wind integration.

2.3 Conventional Governor and Load Frequency Control

The classical theory of speed governing and load frequency control is presented in the textbooks of Kundur [7] and Glover and Sarma [8]. In these models the generator–load dynamics are represented by the swing equation with a damping term, and the governor is modelled by a droop characteristic followed by actuator and prime-mover time constants. Ibraheem *et al.* [10] reviewed the philosophies of automatic generation control, covering classical integral and PI controllers, optimal and adaptive control and the first intelligent approaches. Pandey *et al.* [11] extended the survey to systems with distributed generation and highlighted that fixed-gain controllers tuned for a nominal operating point lose performance when the system parameters change, a situation that arises naturally when renewable generation varies. Bevrani [9] and Bevrani and Hiyama [29] presented robust and intelligent formulations of frequency control and argued that controllers able to adapt their effective gain to the size of the disturbance are better suited to systems with high renewable penetration.

For isolated micro-grids, Peças Lopes *et al.* [30] defined control strategies for islanded operation and showed that a single master unit with a fast isochronous controller, supported by droop-controlled sources, is a practical arrangement. In diesel-based islands the master role is played by the diesel governor, which is usually a PI or PID controller with filtering, actuator and engine dead time, exactly as in the San Cristóbal model used in this thesis [18].

3.SYSTEM DESCRIPTION AND MODELLING

3.1 Introduction

This chapter describes the isolated power system studied in the thesis and the mathematical models of its components. The system is based on the electrical network of San Cristóbal Island in the Galápagos archipelago [17, 18]. It consists of three 800 kW wind turbines, three synchronous diesel generators rated at 813 kVA, a composite load and a controllable EV charging aggregate. The complete model is implemented in MATLAB/Simulink using the Specialized Power Systems library of Simscape Electrical [48], and is run at 1 kV; passive elements such as transformers, cables and lines are neglected. The general arrangement of the model, consisting of three subsystems — synchronous generation, wind generation and load — is shown in Fig. 3.1, and the corresponding single-line diagram is given in Fig. 3.2.

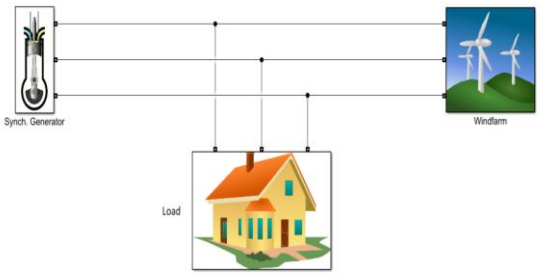


Fig. 3.1: General diagram of the power system model with its three subsystems

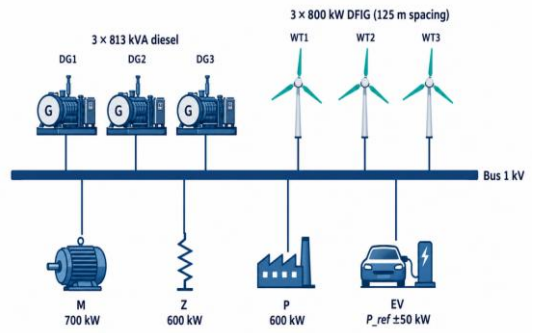


Fig. 3.2: Single-line diagram of the San Cristóbal wind–diesel–EV system3.5 Wind Data and Scenarios

High-resolution wind data are essential for this type of study because the frequency of a low-inertia system responds to gusts lasting a few seconds. The records from Tjæreborg, Denmark [46], measured at 60 m above ground at 25 samples per second at a coastal location without significant orography, provide suitable data. Each simulation consists of a 600 s period during which the turbines are exposed to the wind profile. Four profiles are selected according to two criteria — mean wind speed U and turbulence index TI — and their statistics are listed in Table 3.4. The time series used in the simulations are plotted in Fig. 3.9.

Table 3.4: Wind data parameters

Wind profile	w1	w2	w4	w5
Mean speed U (m/s)	5.25	11.61	4.61	10.03
Std. deviation SD (m/s)	0.1181	0.6483	0.4973	1.715
Turbulence index TI (%)	2.25	5.58	10.8	17.09
U_{min} (m/s)	4.84	9.85	2.77	6.13
U_{max} (m/s)	5.68	13.93	6.23	13.53
Classification	Low U, low TI	High U, low TI	Low U, high TI	High U, high TI

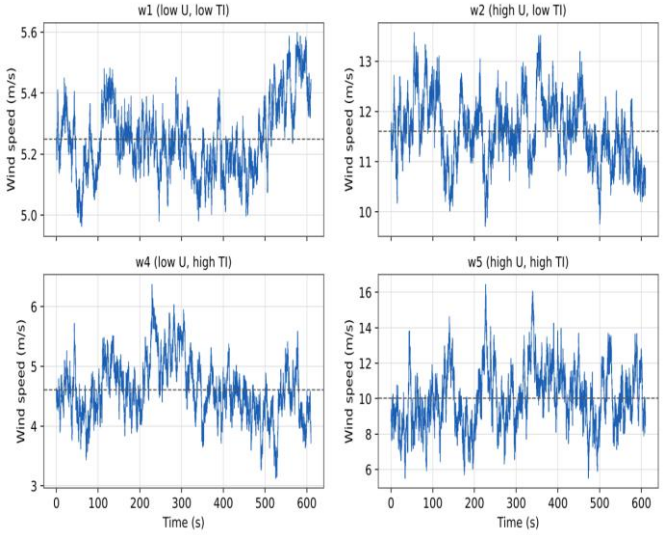


Fig. 3.9: Wind speed profiles used in the simulations (600 s, 25 samples/s); dashed lines show the mean speed

All scenarios have the same total base load of 1900 kW. At low wind speed (w1, w4) three turbines produce about 200 kW and the diesel generation supplies 1700 kW; at high wind speed (w2, w5) two turbines produce about 1600 kW and the diesel generation only 300 kW, giving a wind penetration of 84 %. The scenario data are summarised in Table 3.5.

Table 3.5: Data for the studied scenarios

Parameter	Symbol	Low wind (w1, w4)	High wind (w2, w5)
Wind turbines in service	n_{DFIG}	3	2
Wind power generation	P_W	200 kW	1600 kW
Diesel generation	P_{GS}	1700 kW	300 kW
Rated power of AM	S_{AM}	1500 kW	1500 kW
Induction motor load	P_{AM}	700 kW	700 kW
Constant impedance load	P_Z	600 kW	600 kW
Constant power load	P_S	600 kW	600 kW
Wind penetration	P_W/P_L	10.50%	84.20%

3.6 Load Subsystem

The load subsystem, shown in Fig. 3.10, has two groups: the conventional load and the EV charging load.

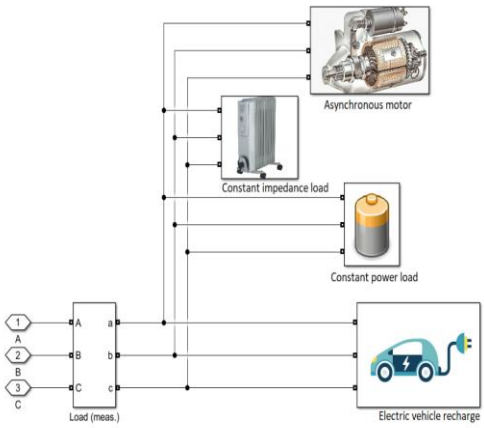


Fig. 3.10: Simulink model of the load subsystem

3.6.1 Conventional load

The conventional load is a combination of three types, each absorbing about one third of the total demand:

- Constant power loads, demanding a constant active power P and no reactive power.
- Constant impedance (Z) loads, whose power varies with the square of the voltage.
- Inertial loads, consisting of an equivalent asynchronous motor with an inertia constant of 0.5 s and rated power S_{AM}, operated at half load; its reactive power is partially compensated by a capacitive load providing 30 % of S_{AM}.

The asynchronous motor is the main source of frequency-dependent load behaviour and contributes to both the inertia in (3.3) and the damping D in (3.2).

4.FUZZY LOGIC CONTROLLER DESIGN

4.1 Introduction

This chapter presents the theory of fuzzy logic control and the step-by-step design of the fuzzy governor that replaces the PI governor of the diesel generation. The design follows the classical Mamdani approach [20, 21]: the frequency deviation and its rate of change are converted into linguistic variables, a rule base expresses the control strategy of an experienced operator, and the inferred fuzzy action is converted back into a crisp governor signal. The resulting controller is nonlinear, uses derivative information that the PI governor ignores, and adapts its effective gain to the size and direction of the disturbance.

5.MATLAB/SIMULINK IMPLEMENTATION

5.1 Introduction

This chapter describes how the system of Chapter 3 and the fuzzy governor of Chapter 4 are implemented and simulated in MATLAB/Simulink. The work flow of the complete study is shown in Fig. 5.1. The model is first built and validated with the original PI governor, the fuzzy inference system is then created with the Fuzzy Logic Toolbox [45], and finally the governor subsystem is replaced while every other block of the model is left unchanged, so that the comparison between the two governors is fair.

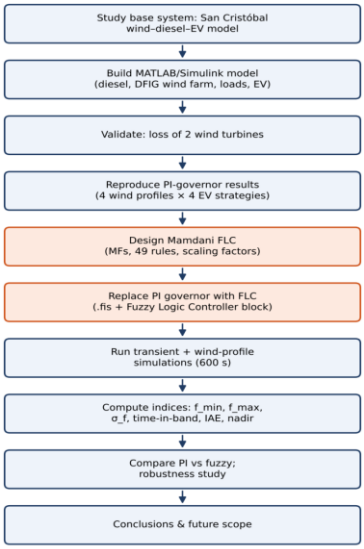


Fig. 5.1: Methodology flowchart of the simulation study

5.2 Simulink Model of the Complete System

The top level of the Simulink model is shown schematically in Fig. 5.2. It contains the *powergui* block configured for phasor simulation at 60 Hz, the diesel generator (Synchronous Machine pu Standard block with excitation system), the governor subsystem, the diesel engine and actuator, the three-phase measurement at the 1 kV bus, the wind farm subsystem of Fig. 3.7, the load subsystem of Fig. 3.10 including the EV recharge block, the wind profile source and the logging blocks.

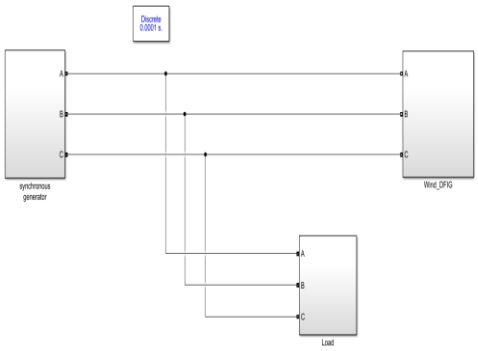


Fig. 5.2: Top-level Simulink model of the wind–diesel–EV system with the fuzzy governor subsystem

The main modelling choices are:

- **Diesel unit.** One equivalent synchronous machine with the parameters of Table 3.1. The mechanical power input P_m is computed from the governor output torque multiplied by the rotor speed, as in (3.6).
- **Wind farm.** Three averaged DFIG models (*wind_dfig_avg*), each with its own breaker, driven by the wind profile delayed according to (3.8). The breakers allow the loss of turbines to be simulated for the validation event.
- **Loads.** A three-phase dynamic load (constant power), a series RLC load (constant impedance), and an asynchronous machine with a mechanical load torque equal to half its rating.
- **EV recharge.** A controlled active-power load whose set point is $P_{EVref} + \Delta P_{EV}(\Delta f)$; the function ΔP_{EV} is implemented with a MATLAB Function block selecting the proportional, soft or aggressive characteristic of (3.10) – (3.12), or zero for the no-EV case.
- **Measurement.** The frequency is obtained from the rotor speed of the synchronous machine, which in this single-bus model is equal to the bus frequency; the same locally measured signal is used by the governor and by the EV controller.

5.3 Creating the Fuzzy Inference System

The fuzzy inference system (FIS) *gov_flc* is created with a MATLAB script using the object-based functions of the Fuzzy Logic Toolbox (*mamfis*, *addInput*, *addMF*, *addOutput* and *addRule*). The full script is listed in Appendix A. The script defines the two inputs and the output on the range [−1, 1], adds the seven triangular membership functions of Table 4.1 to each variable, builds the 49 rules of Fig. 4.6 from the rule matrix, sets the min/max operators and centroid defuzzification, and saves the system with *writeFIS* as *gov_flc.fis*.

The resulting system can be opened in the Fuzzy Logic Designer to inspect and edit it graphically, as represented in Fig. 5.3. The

Membership Function Editor, Rule Editor, Rule Viewer and Surface Viewer of the toolbox correspond to Fig. 4.5, Fig. 4.6, Fig. 4.7 and Fig. 4.8 respectively.

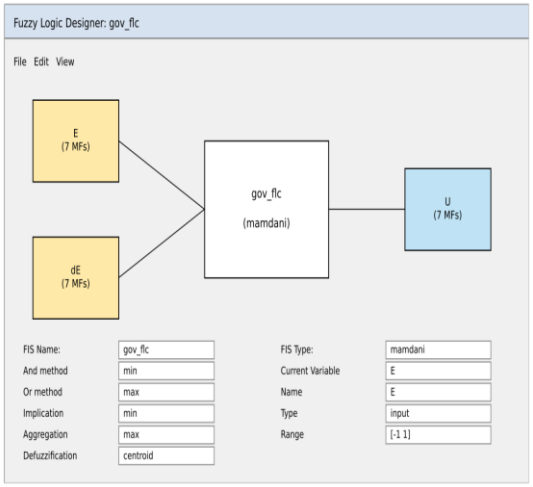


Fig. 5.3: Fuzzy Logic Designer view of the governor FIS (two inputs, Mamdani type, one output)

Table 5.1: Simulation settings

Setting	Value
Software	MATLAB/Simulink, Simscape Electrical (Specialized Power Systems), Fuzzy Logic Toolbox
Simulation type	Phasor / discrete, fixed step
Step size	5 ms
Wind-profile run length	600 s (+60 s initialisation discarded)
Transient test length	30 s, event at t = 5 s
Wind data rate	25 samples/s (Tjæreborg, 60 m height)
Wind incidence angle	φ = 60° (turbine-to-turbine delay 125·sin φ / U_m)
System base	2439 kVA (3 × 813 kVA), 1 kV, 60 Hz
Acceptable band	60 ± 0.15 Hz (0.25 %)
Total cases	4 wind profiles × 4 EV strategies × 2 governors = 32

6.SIMULATION RESULTS AND DISCUSSION

6.1 Introduction

This chapter presents the simulation results obtained with the PI governor of the base system and with the proposed fuzzy governor. Three groups of tests are carried out: transient events (the loss of two wind turbines and load steps of ±100 kW), 600 s simulations with the four turbulent wind profiles combined with the four EV conditions, and a robustness study in which key system parameters are varied. In all figures the PI governor is drawn in blue and the fuzzy governor in orange. All results are from simulation; no experimental data are involved.

6.2 Validation Event: Loss of Two Wind Turbines

The first test reproduces the event used to validate the San Cristóbal model [18]: with 600 kW of wind generation from three turbines, two turbines are disconnected at t = 5 s, so that about 400 kW of generation is lost within the response time of the DFIG controls. The frequency and the diesel power are shown in Fig. 6.1 and the indices are listed in Table 6.1.

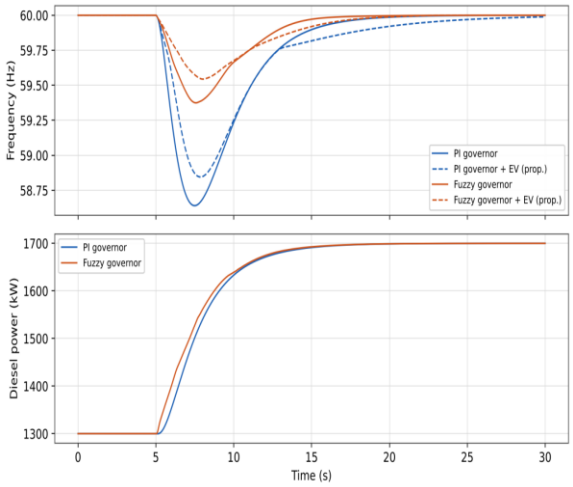


Fig. 6.1: Loss of two wind turbines at t = 5 s: frequency (top) and diesel mechanical power (bottom) with PI and fuzzy governors, with and without proportional EV response

With the PI governor the frequency falls to 58.64 Hz, a deviation of 1.36 Hz, before the integral action restores it; the shape of the response — a fast drop, a nadir after about 2.5 s and a slow recovery — agrees with the recorded event in [18] and confirms that the model captures the dominant dynamics. The fuzzy governor detects the high rate of change of frequency immediately through its ΔE input and increases the fuel admission earlier, as visible in the steeper initial rise of the diesel power. The nadir is raised to 59.38 Hz (54 % smaller deviation), the settling time to ±0.02 Hz falls from 14.1 s to 10.6 s, and the IAE is reduced by

57 %. Adding the proportional EV response further reduces the deviation for both governors; the best result, 59.54 Hz, is obtained with the fuzzy governor and EV participation together.

Table 6.1: Response indices for the loss of two wind turbines

Case	Index	PI	Fuzzy	Improvement
No EV	Peak deviation |Δf| (Hz)	1.359	0.625	54.00%
	Extreme frequency (Hz)	58.641	59.375	–
	Settling time to ±0.02 Hz (s)	14.06	10.64	24.30%
	IAE (Hz·s)	6.748	2.93	56.60%
Proportional EV	Peak deviation |Δf| (Hz)	1.155	0.456	60.50%
	Extreme frequency (Hz)	58.845	59.544	–
	Settling time to ±0.02 Hz (s)	22.16	13.64	38.40%
	IAE (Hz·s)	6.727	2.696	59.90%

6.3 Load Step Tests

To evaluate the governors under a controlled disturbance, a sudden load increase of 100 kW (about 5 % of the demand) and a sudden load decrease of the same size are applied at t = 5 s in the low-wind condition. The responses are shown in Fig. 6.2 and Fig. 6.3 and the indices in Table 6.2 and Table 6.3.

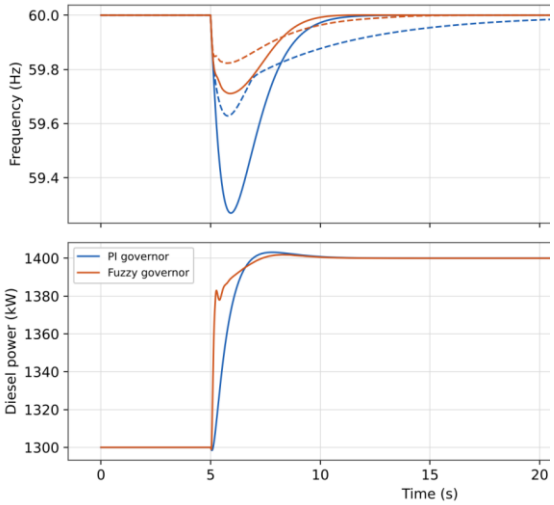


Fig. 6.2: Response to a 100 kW load increase at t = 5 s

Table 6.2: Response indices for a 100 kW load increase

Case	Index	PI	Fuzzy	Improvement
No EV	Peak deviation |Δf| (Hz)	0.731	0.289	60.40%
	Extreme frequency (Hz)	59.269	59.711	–
	Settling time to ±0.02 Hz (s)	5.28	4.41	16.40%
	IAE (Hz·s)	1.687	0.752	55.40%
Proportional EV	Peak deviation |Δf| (Hz)	0.372	0.177	52.40%
	Extreme frequency (Hz)	59.628	59.823	–
	Settling time to ±0.02 Hz (s)	14.18	6.23	56.00%
	IAE (Hz·s)	1.687	0.613	63.70%

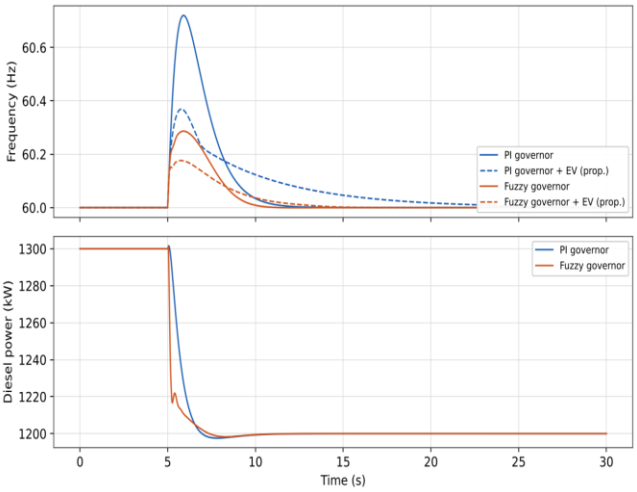


Fig. 6.3: Response to a 100 kW load decrease at t = 5 s

Table 6.3: Response indices for a 100 kW load decrease

Case	Index	PI	Fuzzy	Improvement
No EV	Peak deviation |Δf| (Hz)	0.72	0.286	60.20%
	Extreme frequency (Hz)	60.72	60.286	–
	Settling time to ±0.02 Hz (s)	5.54	4.45	19.60%
	IAE (Hz·s)	1.687	0.748	55.60%
Proportional EV	Peak deviation |Δf| (Hz)	0.369	0.176	52.20%
	Extreme frequency (Hz)	60.369	60.176	–
	Settling time to ±0.02 Hz (s)	14.27	6.25	56.20%
	IAE (Hz·s)	1.687	0.612	63.70%

The initial rate of change of frequency is identical for both governors (about 1.69 Hz/s), because it is fixed by the inertia of the system and the size of the step ($\Delta P/2H_s$); no governor can act within the first tens of milliseconds owing to the engine dead time. Thereafter the fuzzy governor arrests the frequency much sooner: the peak deviation is reduced from 0.73 Hz to 0.29 Hz (60 %) for the load increase and from 0.72 Hz to 0.29 Hz for the load decrease, and the IAE is reduced by about 55 %. The responses for increase and decrease are almost symmetrical, confirming that the odd-symmetric rule base treats under- and over-frequency equally. An interesting observation concerns the IAE of the PI governor, which is the same with and without EV participation (1.687 Hz·s). This is a property of integral control without overshoot: the integral of the error must equal the change of the integrator

state divided by K_I, which is fixed by the size of the step. EVs reduce the peak of the deviation but spread it over a longer time, which is also why the settling time with the PI governor and EVs is longer (14.2 s). With the fuzzy governor the extra proportional and derivative action breaks this constraint and both the peak and the IAE are reduced.

6.4 Wind-Profile Simulations with the PI Governor

6.4.1 Wind power fluctuations

The wind farm output produced by the four profiles is shown in Fig. 6.4. For the low-wind profiles the output fluctuates around 200 kW with a standard deviation of about 11 kW (w1) and 45 kW (w4). For the high-wind profiles the turbines operate close to their rated power and the pitch control limits the output during gusts, but every lull below rated speed causes a deep drop: the standard deviation of the wind power is 93 kW for w2 and 224 kW for w5, and in w5 the output falls to about 520 kW at the deepest lulls. These fluctuations, of the order of 5–12 % of the system demand, act as a continuous disturbance on the island frequency.

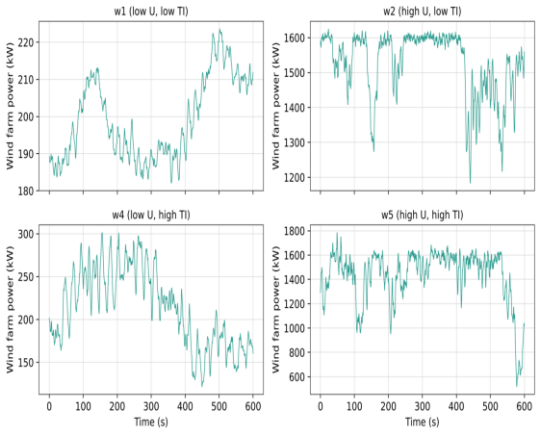


Fig. 6.4: Wind farm active power for the four wind profiles

6.7.1 Quantitative comparison

The main quantitative comparison between the two governors is presented in Table 6.7 and in Fig. 6.15, for the cases without EVs and with proportional EV response.

Table 6.7: Comparison of PI and fuzzy governors (σ_f, maximum frequency dip and time within band)

Profile	EV	σ_f PI	σ_f Fuzzy	$\Delta\sigma_f$	Max dip PI (Hz)	Max dip Fuzzy (Hz)	In-band PI (%)	In-band Fuzzy (%)
w1	No EV	0.0154	0.004	74.30%	0.05	0.013	100	100
	Proportional	0.0119	0.004	66.80%	0.028	0.012	100	100
w2	No EV	0.2473	0.0918	62.90%	1.027	0.425	63.9	89.3
	Proportional	0.1529	0.0646	57.80%	0.959	0.337	78.4	95.7
w4	No EV	0.1026	0.0264	74.30%	0.264	0.071	84.2	100
	Proportional	0.0573	0.0227	60.40%	0.132	0.055	99.9	100
w5	No EV	0.5714	0.2636	53.90%	2.134	1.308	27.4	56.8
	Proportional	0.4208	0.1902	54.80%	1.814	0.958	50.5	72.1

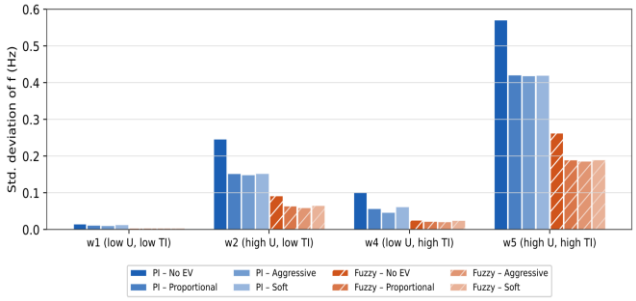


Fig. 6.15: Standard deviation of frequency for all governors, EV strategies and wind profiles

The fuzzy governor improves every index in every scenario. The reduction of σ_f ranges from 54 % (w5) to 74 % (w1 and w4) without EVs, and from 55 % to 67 % with proportional EV response. The maximum frequency dip is reduced from 0.050 Hz to 0.013 Hz for w1, from 1.03 Hz to 0.43 Hz for w2 and from 2.13 Hz to 1.31 Hz for w5. Notably, the fuzzy governor without any EV participation performs better than the PI governor with the best EV strategy in every profile (for example σ_f = 0.092 Hz against 0.149 Hz for w2, and 0.264 Hz against 0.419 Hz for w5).

6.7.2 Diesel power and EV utilisation

Fig. 6.16 shows the diesel mechanical power and the EV power modulation for profile w5 with proportional EV response. The diesel power varies between about 180 kW and 1330 kW with both governors, with practically the same standard deviation (213 kW and 215 kW), because in both cases the diesel unit must ultimately compensate the slow wind-power fluctuations. The difference lies in the timing: the fuzzy governor reacts earlier to each change

and therefore avoids the large frequency deviations that accumulate while the PI governor is still responding. As a consequence the EV aggregate is used less intensively: its modulation is at the ±50 kW limit 32 % of the time with the PI governor but only 14 % of the time with the fuzzy governor, and the standard deviation of ΔP_{EV} falls from 34 kW to 26 kW. The fuzzy governor thus not only improves the frequency but also reduces the service demanded from the EV owners.

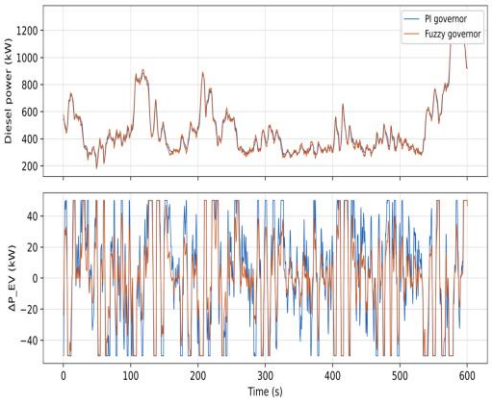


Fig. 6.16: Diesel mechanical power (top) and EV power modulation (bottom) for profile w5 with proportional EV response

6.7.3 Qualitative comparison

A qualitative comparison of the two governors, drawing on all the results, is given in Table 6.8.

Table 6.8: Qualitative comparison of PI and fuzzy governors

Aspect	PI governor	Fuzzy governor
Design basis	Linear model, fixed gains	Expert rules, linguistic variables
Non-linearity handling	None (single operating point)	Inherent, gain varies with |Δf| and dΔf/dt
Derivative information	Not used	Used (rate of change input)
Tuning effort	Two gains	Three scaling factors + MFs + rules
Computational load	Very low	Low (surface look-up)
Response to small wind noise	Slow, low gain	Fast, smooth
Response to large events	Deep nadir	Nadir reduced 52–60 %
Robustness (±30 % H, 2× delay)	Degrades	Nearly unchanged
Interaction with EV response	EVs provide most of the benefit	EVs give additional 25–30 % σ_f reduction at high wind

6.8 Robustness to Parameter Variations

The parameters of an isolated system change with the number of diesel units in service, with the composition of the load and with ageing of the engine. To test robustness, both governors — with unchanged gains and scaling factors — were simulated with the system inertia reduced and increased by 30 %, with the engine dead time doubled, and with the load damping reduced by 50 %. The 100 kW load step and the turbulent profile w4 were used. The results are shown in Fig. 6.17 and Table 6.9.

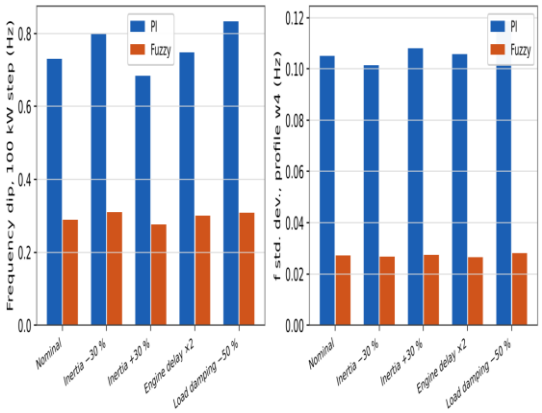


Fig. 6.17: Robustness study: frequency dip for a 100 kW step and σ_f for profile w4 under parameter variations

Table 6.9: Results of the robustness study

Parameter case	Dip PI (Hz)	Dip Fuzzy (Hz)	σ_f w4 PI (Hz)	σ_f w4 Fuzzy (Hz)
Nominal	0.731	0.289	0.1051	0.0272
Inertia −30 %	0.8	0.309	0.1015	0.0268
Inertia +30 %	0.685	0.276	0.1081	0.0274
Engine delay ×2	0.748	0.301	0.1057	0.0266
Load damping −50 %	0.833	0.308	0.1186	0.028

The PI governor is sensitive to the parameter changes: its frequency dip ranges from 0.69 Hz to 0.83 Hz, and σ_f for w4 increases to 0.119 Hz when the load damping is halved. The fuzzy governor keeps the dip between 0.28 Hz and 0.31 Hz and σ_f between 0.027 Hz and 0.028 Hz in all cases. The worst case of the fuzzy governor is better than the best case of the PI governor for both indices.

6.9 Discussion

The results consistently show that the fuzzy governor is superior to the fixed-gain PI governor in this low-inertia, high-wind island system. Three mechanisms explain the improvement. First, the fuzzy controller uses the rate of change of frequency, which in a system with an inertia of only 0.73 s is the earliest indicator of a power imbalance; the PI governor waits until the frequency error itself has grown. Second, near equilibrium the fuzzy governor has a higher effective gain than the PI governor (Section 4.4.6), which suppresses the small, frequent fluctuations caused by turbulence. Third, the shape of the rule base and the control surface reduces the incremental gain for large deviations and when the frequency is already recovering, which avoids overshoot and actuator saturation and makes the response robust.

It should be noted that part of the improvement comes from the higher equivalent small-signal gains of the fuzzy controller and its derivative action, and that a PI or PID governor re-tuned for this system would recover part of the benefit. The base PI parameters were deliberately kept unchanged because they represent the governor actually used in the reference system [17, 18]. A comparison with an optimally tuned PID governor is therefore identified as future work. The robustness results suggest, however, that the nonlinear fuzzy design maintains its performance over a range of operating conditions where a fixed linear controller tuned for one point would not.

The results also confirm the main conclusion of the base study from a new angle: demand-side EV participation and generation-side control are complementary. With the PI governor, EVs provide most of the improvement; with the fuzzy governor, the governor provides most of it and EVs add a further 25–30 % at high wind while being activated less often. Even the best combination does not keep the frequency inside the band at all times for w5, where the wind penetration exceeds 80 % and the wind power drops by more than 1 MW within seconds. Such conditions call for additional resources, for example a larger EV share, battery storage [38] or frequency support from the wind turbines themselves [28].

6.10 Summary

The fuzzy governor reduced the frequency deviation after the loss of two wind turbines by 54 % and after ±100 kW load steps by about 60 %, reduced the standard deviation of frequency by 54–74 % in all 16 wind-profile and EV combinations, and increased the time within 60 ± 0.15 Hz to 100 % for w4, 97.2 % for w2 and 75.5 % for w5 when combined with aggressive EV control. Its performance was practically unaffected by ±30 % inertia changes, a doubled engine dead time and a halved load damping.

7.1 Conclusions

This thesis has extended the study of electric vehicle recharge strategies for frequency control in the isolated wind–diesel power system of San Cristóbal Island [17] by replacing the conventional PI speed governor of the diesel generation with a Mamdani fuzzy logic controller. The complete system — diesel generator and governor, DFIG wind farm driven by measured high-resolution wind data, composite load and a 50 kW frequency-responsive EV charging aggregate — was modelled in MATLAB/Simulink, and the PI and fuzzy governors were compared by simulation under transient events, four turbulent wind profiles with four EV conditions, and parameter variations. The main conclusions are:

- The isolated system has a very low equivalent inertia of about 0.73 s and a wind penetration of up to 84 %; with the base PI governor its frequency is highly sensitive to wind turbulence, and EV participation alone cannot keep it within 60 ± 0.15 Hz at high wind speed, confirming the findings of the base study.
- The designed fuzzy governor — two inputs (frequency error and its rate of change), seven triangular membership functions per variable, 49 rules, min–max inference, centroid defuzzification and an incremental structure with integral action — is a drop-in replacement for the PI governor and preserves zero steady-state error.
- After the loss of two wind turbines the frequency nadir improved from 58.64 Hz to 59.38 Hz (54 % smaller deviation) and the IAE was reduced by 57 %. For ±100 kW load steps the peak deviation was reduced by about 60 % and the IAE by about 55 %.
- For the 600 s wind profiles the fuzzy governor reduced the standard deviation of frequency by 54–74 % in every wind profile and EV condition, and the fuzzy governor without EVs outperformed the PI governor with the best EV strategy in all profiles.
- The time within the acceptable band rose from 84.2 % to 100 % for w4 and from 63.9 % to 89.3 % for w2 without EVs; with aggressive EV control it reached 97.2 % for w2 and 75.5 % for w5, against 83.2 % and 56.4 % with the PI governor.
- Generation-side fuzzy control and demand-side EV response are complementary: EVs add a further 25–30 % reduction of σ_f at high wind, while with the fuzzy governor they reach their power limit far less often (14 % instead of 32 % of the time for w5).
- As in the base study, the differences between the proportional, soft and aggressive EV strategies are small compared with the effect of having demand response; the aggressive strategy gives the best results at high wind.
- The fuzzy governor was robust: with ±30 % inertia, doubled engine dead time and halved load damping its performance changed by less than 10 %, and its worst case remained better than the best case of the PI governor.

7.2 Future Scope

The work can be continued in the following directions:

- Comparison with an optimally tuned PID governor and with self-tuning fuzzy-PI or adaptive neuro-fuzzy (ANFIS) governors, and optimisation of the membership functions and scaling factors by metaheuristic algorithms.
- A fuzzy or adaptive controller for the EV aggregate itself, including the battery state of charge, charger limits and user requirements [32, 35].
- Coordination of the fuzzy governor and EV response with synthetic inertia and primary frequency support from the wind turbines [28] and with battery energy storage [38].
- Inclusion of other perturbations such as photovoltaic generation, and of voltage and reactive power control.
- Real-time hardware-in-the-loop validation of the fuzzy governor, and quantification of the financial and environmental impact of the combined approach.

REFERENCES

[1] H. Ibrahim, M. Ghandour, M. Dimitrova, A. Ilinca, and J. Perron, “Integration of wind energy into electricity systems: Technical challenges and actual solutions,” Energy Procedia, vol. 6, pp. 815–824, 2011.

[2] R. Pena, J. C. Clare, and G. M. Asher, "Doubly fed induction generator using back-to-back PWM converters and its application to variable-speed wind-energy generation," IEE Proc.—Electric Power Applications, vol. 143, no. 3, pp. 231–241, May 1996.

[3] A. Ulbig, T. S. Borsche, and G. Andersson, "Impact of low rotational inertia on power system stability and operation," IFAC Proceedings Volumes, vol. 47, no. 3, pp. 7290–7297, 2014.

[4] P. Tielens and D. Van Hertem, "The relevance of inertia in power systems," Renewable and Sustainable Energy Reviews, vol. 55, pp. 999–1009, 2016.

[5] J. G. Slootweg and W. L. Kling, "The impact of large scale wind power generation on power system oscillations," Electric Power Systems Research, vol. 67, no. 1, pp. 9–20, 2003.

[6] T. Ackermann, Ed., Wind Power in Power Systems. Chichester, U.K.: Wiley, 2005.

[7] P. Kundur, Power System Stability and Control. New York, NY, USA: McGraw-Hill, 1994.

[8] J. D. Glover and M. S. Sarma, Power System Analysis and Design, 3rd ed. Pacific Grove, CA, USA: Wadsworth/Thomson Learning, 2002.

[9] H. Bevrani, Robust Power System Frequency Control, 2nd ed. Cham, Switzerland: Springer, 2014.

[10] Ibraheem, P. Kumar, and D. P. Kothari, "Recent philosophies of automatic generation control strategies in power systems," IEEE Trans. Power Syst., vol. 20, no. 1, pp. 346–357, Feb. 2005.